ELSEVIER

Journal of Organometallic Chemistry 515 (1996) 233–243

Journal of Organometallic Chemistry

Insertion into the nickel–carbon bond of N–O chelated arylnickel(II) complexes. The development of single component catalysts for the oligomerisation of ethylene

Sylvie Y. Desjardins [a], Kingsley J. Cavell [a,*], Hong Jin [a], Brian W. Skelton [b], Allan H. White [b]

[a] *Department of Chemistry, University of Tasmania, Hobart, Tas. 7001, Australia*
[b] *Department of Chemistry, University of Western Australia, Nedlands, W.A. 6907, Australia*

Received 30 October 1995

Abstract

A series of arylnickel phosphine complexes containing chelating N–O ligands, of the type [NiAr(N–O)L] [N–O = pyridine carboxylate (pyca); Ar = *o*-tolyl; L = PPh_3, $P(CH_2Ph)_3$, $PMePh_2$, PMe_2Ph, PCy_3: R = *p*-tolyl; L = PPh_3: Ar = phenyl; L = PPh_3: R = mesityl; L = $PMePh_2$: N–O = pyridine acetate (pyac); Ar = mesityl; L = $PMePh_2$] have been prepared, providing complexes with chelate ring sizes of five and six. Crystal structures for the complexes indicate that both complexes have "square planar" coordination about the nickel centre, with the nitrogen of the pyridine being *trans* to the phosphine in each case. Whereas significant bending and buckling of the six-membered chelate ring is evident for [Ni(mesityl)(pyac)$PMePh_2$], the five-membered ring of [Ni(mesityl)(pyca)$PMePh_2$] is essentially planar. On warming the complexes readily insert ethylene into the Ni–aryl bond, forming single component catalysts for the conversion of ethylene into higher oligomers with low to moderate activity. Products are linear with generally 60–80% having the double bond in the α-position. Catalyst activities and product distributions are markedly dependent on the phosphine present. Addition of excess PPh_3 to the catalyst [Ni(*o*-tolyl)(pyca)PPh_3] leads to a marked change in the product distribution with a less dramatic change in catalyst activity. A possible mechanism in which ethylene insertion occurs via an associative pathway from a five coordinate intermediate, [NiAr(CH_2=CH_2)(pyca)PR_3], is suggested.

Keywords: Nickel; Olefin insertion; Arylnickel complexes; Synthesis; Crystal structure; C–C bond formation; Catalysis

1. Introduction

Metal complexes containing "hemilabile" bidentate ligands have attracted considerable attention, particularly in their application to the modelling and development of catalytic systems [1–7]. The belief is that a partially labile chelate ligand would sequentially protect and then liberate a vacant site, allowing the catalytic process to proceed in a controlled manner. Insertion reactions, which are important in many catalytic reactions, are thought to occur via an associative or dissociative process, depending on the ligands co-ordinated to the metal centre. For many complexes containing chelating ligands, insertion from a planar, four-coordinate intermediate is favoured, i.e. via a dissociative route. For such systems, ligand lability, either of the chelate ligand or of an associated monodentate ligand, is a necessary requirement for insertion [7].

We have carried out detailed investigations on the CO and alkene insertion behaviour of hydrocarbyl chelate complexes of palladium(II) and platinum(II) [3,4,7,8]. Recent fundamental studies have looked at hydrocarbyl complexes containing bidentate anionic ligands of the type N–O [primarily pyridine carboxylate (pyca, **I**) and related ligands], and a monodentate ligand L (generally a phosphine) [4,7,8]. We have shown that in hydrocarbyl–palladium(II) and platinum(II) complexes containing pyca, ligand dissociation/displacement is extremely facile. The platinum complexes [PtMe(pyca)PPh_3] and [PtEt(pyca)PPh_3] in particular are unusually reactive. Carbonylation/decarbonylation

* Corresponding author.

SSDI 0022-328X(95)06105-3

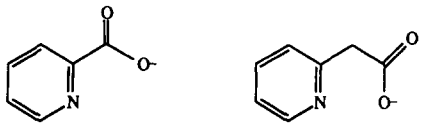

pyridine carboxylate (pyca) pyridine acetate (pyac)

I II

Form 1.

of the methyl complex occurs under very mild conditions, and the ethyl complex readily eliminates ethylene on warming to give platinum-hydrides [4]. Small changes to the pyca ligand can cause major changes in the CO insertion pathway, and hemilability of the N–O chelate is clearly indicated [7,9], illustrating the potential control available in developing catalysts based on complexes containing these types of ligand.

Subsequent to the modelling studies we have now developed nickel catalyst species containing N–O (pyca type ligands). Recently, examples of alkylnickel complexes containing pyca were reported [10]. Preparative procedures for the alkyl complexes were relatively difficult and not generally applicable, and no catalysis with these complexes was reported. In this paper we describe the preparation and characterisation of a range of new arylnickel complexes containing the N–O chelates **I** and **II**. The complexes are single component catalysts for the conversion of ethylene to higher oligomers. Analysis of primary reaction products from initial ethylene insertions and catalysis with [Ni(*o*-tolyl(pyca)PPh_3)] in the presence of various amounts of excess triphenylphosphine has provided useful mechanistic information. The application of related complexes for the formation of polyethylene and polyketones will be reported in a forthcoming publication.

Crystal structure analyses of the complexes [Ni(mesityl)(pyca)$PMePh_2$] and [Ni(mesityl)(pyac)-$PMePh_2$] are also reported herein. These studies afford an opportunity to assess structural effects correlated with changes to the N–O to nickel chelate ring.

2. Experimental

Experimental manipulations were generally carried out under dry, oxygen free nitrogen using Schlenk apparatus and standard vacuum line procedures, unless otherwise stated. Solvents were dried and purified by standard methods and freshly distilled before use. Other reagents were used as received. The complexes [$NiX_2(L)_2$]; (X = Cl, Br; L = PPh_3, PCy_3, $P(CH_2Ph)_3$, PMe_2Ph, $PMePh_2$) were prepared by published methods [11,12].

Nuclear magnetic resonance spectra were recorded at 22°C on a Bruker AM-300 NMR spectrometer at 300.13 MHz (^1H), 75.48 MHz (^{13}C), and 121.50 MHz (^{31}P), or a Varian Gemini-200 at 199.98 MHz (^1H). Solutions for the NMR were prepared in $CDCl_3$ or deuterated benzene and pulsed in a 5 mm probe. Chemical shifts δ are reported in parts per million relative to internal $(CH_3)_4Si$ (^1H, ^{13}C) or external 85% H_3PO_4 (^{31}P). Coupling constants J are given in hertz and NMR peaks are given as singlet (s), doublet (d), triplet (t) and multiplet (m). Unlabelled NMR peaks can be assumed to be singlets.

Infrared spectra were recorded on a Hitachi 270-30 IR spectrophotometer. FTIR spectra were recorded on a Bruker IFS-66 FTIR spectrometer. Potassium bromide disks were used in the mid IR range (4000–400 cm^{-1}). Bands (cm^{-1}) were described as strong (s), medium (m) or weak (w) in intensity.

Microanalyses were carried out by the Central Science Laboratory (University of Tasmania) on a Carlo Erba CHNS-O EA elemental analyser.

2.1. Structure determinations

Unique room-temperature diffractometer data sets ($T \sim 295$ K; monochromatic Mo Kα radiation, $\lambda = 0.7107_3$ Å; $2\theta/\theta$ scan mode; $2\theta_{max} = 50°$) were measured, yielding N independent reflections, N_o with $I > 3\sigma(I)$ being considered "observed" and used in the full-matrix least-squares refinements after Gaussian absorption correction. Anisotropic thermal parameters were refined for the non-hydrogen atoms, (x, y, z, $U_{iso})_H$ being constrained at estimated values. Conventional residuals on $|F|$ at convergence R, R_w are quoted; statistical weights were derivative of $\sigma^2(I) = \sigma^2(I_{diff}) + 0.0004\sigma^4(I_{diff})$. Neutral atom complex scattering factors were employed, with computation using the XTAL 3.2 program system implemented by Hall [13]. Pertinent results are given in the figures and tables. Tables of structure factor amplitudes, thermal and hydrogen atom parameters and complete lists of bond lengths and angles have been deposited at the Cambridge Crystallographic Data Centre.

2.1.1. Crystal / refinement data

[Ni(mesityl)(pyca)$(PMePh_2)$] = $C_{28}H_{28}NNiO_2P$, M = 500.2. Monoclinic, space group $P2_1/c$ (No. 14), a = 14.795(11), b = 8.325(7), c = 21.638(4) Å, β = 106.11(6)°, V = 2560 Å^3, $D_c(Z = 4)$ = 1.30 g cm^{-3}; $F(000)$ = 1048. μ_{Mo} = 8.7 cm^{-1}; specimen: 0.42 × 0.21 × 0.39 mm^3; $A^*_{min,max}$ = 1.14, 1.40. N = 4294, N_o = 2532; R = 0.070, R' = 0.070; n_v = 337.

The precision of the determination was adversely affected by (i) some decomposition, compensated for by scaling based on periodic intensity standards, and (ii) rotational disorder in phenyl ring 12, about the C(121)–C(124) axis. The two components of the other two atoms were assigned site occupancies of 0.5 after trial refinement; it is noticeable that "thermal motion"

throughout the structure is generally appreciably higher than for the pyac analogue, perhaps consequential on the structure being affected throughout by unresolved disorder consequent upon the alternative phenyl ring dispositions or, possibly, an undetected space group problem. Derivative geometries should be treated with some circumspection.

[Ni(mesityl)(pyac)($PMePh_2$)] = $C_{29}H_{30}NNiO_2P$, M = 514.3. Orthorhombic, space group *Pbca* (No. 61), a = 31.517(9), b = 17.671(9), c = 9.419(5) Å, V = 5246 Å^3. $D_c(Z = 8)$ = 1.30 g cm^{-3}; $F(000)$ = 2160. μ_{Mo} = 8.3 cm^{-1}; specimen: 0.32 × 0.14 × 0.43 mm^3; $A^*_{min,max}$ = 1.12, 1.29. N = 4307, N_o = 2651; R = 0.042; R' = 0.042; n_v = 307.

2.2. Synthesis of the ligand salts Tl(pyca) and Na(pyac)

Tl(pyca) was prepared by refluxing a solution of 2-pyridine carboxylic acid (picolinic acid) (4.03 g; 32.7 mmol) and thallium carbonate (Tl_2CO_3) (7.19 g, 15.3 mmol) in methanol (40 ml) for approximately 30–45 min. The solution was cooled to −15°C and filtered. The product, Tl(pyca), precipitated as a white powder. The reaction was virtually quantitative.

To prepare Na(pyac) the hydrochloride salt of 2-pyridine acetic acid was reacted with 2 mol of sodium ethoxide in dry ethanol to form the sodium salt of the 2-pyridine acetate and NaCl. The sodium 2-pyridine acetate (pyac) was readily isolated pure and characterised. ^{1}H NMR in CD_3OD; δ 3.89 (s, 2H, CH_2), 8.49 (m, 4H, py); IR (KBr, cm^{-1}): 1606s, 1566m, 1462s [ν(C=O and ν(C=C)], 3400 ν(C–H).

2.3. Synthesis of complexes [Ni(aryl)BrL$_2$]

The complexes [NiArX(L)2] (X = Br; Ar = *o*-tolyl, *p*-tolyl, phenyl or mesityl; L = PPh_3, PCy_3 or $P(CH_2Ph)_3$) were prepared by a modification of the procedure of Zembayashi et al. [14] involving the oxidative addition of an aryl halide to Ni^0 generated in situ from NiX_2L_2 complexes using zinc dust and ultrasound. Complexes were synthesised employing a thin wall 100 ml Schlenk flask placed in a Branson 1200 Bransonic ultrasonic cleaning bath (47 KHz and 30 W) at 35°C. The reaction mixture was mechanically stirred. A typical procedure is described for the preparation of Ni(*o*-tolyl)Br(PPh_3)$_2$.

Under a flow of nitrogen the reaction vessel was loaded with bis(triphenylphosphine)dichloronickel(II) (4.5 g, 6.9 mmol), azobisisobutyronitrile (AIBN; 0.11 g) and activated zinc powder (3.0 g, 46.8 mmol; activated by washing with a saturated ammonium chloride solution and then dried in an oven at 100°C for 30 min). *o*-Bromotoluene (1.6 ml, 13.6 mmol) and 25 ml of dry tetrahydrofuran were quickly injected into the reaction vessel through a septum in the side arm. Stirring and ultrasound were then started simultaneously. The reaction mixture was treated with ultrasonic radiation for 20 min. The resulting olive brown slurry was diluted with 15 ml CH_2Cl_2 and suction filtered through Celite (where Ar = phenyl or *p*-tolyl no CH_2Cl_2 was used and all manipulations were performed under nitrogen). Methanol (40 ml) was added to the filtrate to precipitate the yellow *trans*-(*o*-tolyl)bromo(triphenylphosphine)-nickel(II). In some cases refrigeration overnight at −20°C was necessary for crystallisation. The precipitate was then filtered in air and washed with cold methanol (yield 5.1 g, 45%).

Where L = $PMePh_2$ or PMe_2Ph it was necessary to prepare the complexes via a Grignard reagent employing the method of Moss and Shaw [15].

2.4. Synthesis of complexes [Ni(aryl)(N–O)L]

All complexes were synthesised by the same general method from $NiRXL_2$. Where R = *p*-tolyl or phenyl manipulations were performed under nitrogen. A typical procedure is described for the preparation of [Ni(*o*-tolyl)(pyca)PPh_3].

A small excess of the thallium picolinate salt Tl(pyca) (0.91 g, 2.8 mmol) was added to a solution of [Ni(*o*-tolyl)XL_2] (2.7 mmol) in 20–30 ml dry tetrahydrofuran. The solution was stirred overnight at room temperature followed by refluxing for approximately 1 h. The dark yellow–orange solution turns pale yellow as TlBr precipitates. The mixture was cooled and then filtered through Celite to remove TlBr. The reaction mixture was evaporated to dryness under vacuum and the residue was redissolved in a minimum quantity of tetrahydrofuran (10–15 ml) and crystallised by the addition of heptane or hexane (30 ml) and cooling overnight at −20°C. The yellow product was filtered and dried under vacuum (yield 1.29 g, 88%). Microanalysis data for the complexes are given in Table 1 and ^{1}H NMR data are summarised in Table 2.

2.5. Catalytic testing

Catalytic testing was carried out in a 75 ml stainless steel autoclave fitted with a glass liner. The autoclave was magnetically stirred and heated with an oil bath or with a heating jacket controlled by a thermocouple placed between the heater and the autoclave. Reaction temperatures of 60–100°C were employed and ethylene pressures of 35–50 bar were used. Catalysis was allowed to run for between 1 and 12 h.

Typically 10^{-4} mol of catalyst was dissolved in 15 ml benzene. The autoclave was evacuated and flushed with nitrogen then ethylene twice before a solution of the complex was injected. The autoclave was closed and pressurised while the solution was stirred. After several minutes the pressure was adjusted to 35 bar and the

Table 1
Microanalytical data for the nickel complexes

Complex	Microanalysis (%)
1a Ni(*o*-tolyl)(pyca)PPh_3	Found: C, 69.22; H, 4.93; N, 2.72 Calc.: C, 69.08; H, 5.03; N, 2.69
1b Ni(*o*-tolyl)(pyca)-$P(CH_2Ph)_3$	Found: C, 70.92; H, 5.69; N, 2.51 Calc.: C, 70.86; H, 5.61; N, 2.43
1c Ni(*o*-tolyl)(pyca)$PMePh_2$	Found: C, 66.05; H, 5.32; N, 3.11 Calc.: C, 66.23; H, 5.13; N, 2.97
1d Ni(*o*-tolyl)(pyca)PMe_2Ph	Found: C, 61.40; H, 5.48; N, 3.26 Calc.: C, 61.51; H, 5.41; N, 3.42
1e Ni(*o*-tolyl)(pyca)PCy_3	Found: C, 66.82; H, 8.24; N, 2.63 Calc.: C, 67.06; H, 7.54; N, 2.55
1f Ni(phenyl)(pyca)PPh_3	Found: C, 70.80; H, 4.62; N, 2.44 Calc.: C, 69.35; H, 4.65; N, 2.70
1h Ni(mesityl)(pyca)$PMePh_2$	Found: C, 67.83; H, 5.76; N, 2.73 Calc.: C, 67.23; H, 5.64; N, 2.80
2 Ni(mesityl)(pyac)$PMePh_2$	Found: C, 66.98; H, 5.99; N, 2.81 Calc.: C, 67.82; H, 5.89; N, 2.73

Satisfactory carbon analysis for complex **1g** could not be obtained. This complex was characterised spectroscopically only.

heating commenced. After 1 h, the autoclave was removed from the heater and cooled to room temperature. The vessel was then slowly depressurised and 0.4 ml of nonane (internal GC standard) was added. Samples were analysed by GC.

2.6. Product analysis

Gas chromatographic analysis was performed on a Hewlett Packard 5890A gas chromatograph fitted with a SGE 50 m QC3/BP1-1.0 μm capillary column. The initial oven temperature was 35°C with a ramp rate of 10°C min^{-1}. Olefin oligomers were identified by GC-MS. C6 olefin isomers, used in determining product linearity, were separated from the crude sample by distillation and individually resolved on a Siemans Sichromat 3 using a 50 m PONA FS HP capillary column. Separation was achieved with an initial oven temperature of 30°C, an isothermal time of 20 min followed by a ramp rate of 20°C min^{-1}.

3. Results and discussion

3.1. Preparation of the [Ni(aryl)(N–O)PR_3] complexes

The complexes [Ni(aryl)(N–O)L] were readily prepared in moderate to high yield by the reaction of the appropriate N–O chelate salt with *trans*-arylbromobis (phosphine)nickel(II) [Ni(aryl)XL_2] in tetrahydrofuran, according to Scheme 1. Formation and precipitation of TIX drives the reaction to the right. The precursor complex, [Ni(aryl)XL_2], was prepared by a Grignard method or by the use of ultrasound. Preparation of [Ni(aryl)XL_2] by ultrasound, from the complexes [$NiCl_2L_2$] and an arylbromide, gives a mixture of halide species. In this work the halide is removed in the next step and therefore was not of concern. However, if [Ni(aryl)$X(L)_2$] is required as either the pure bromide or pure chloride, the appropriate halide must be used for both the [$NiX_2(L)_2$] complex and the arylhalide.

Unlike the hydrocarbylpalladium(II) and platinum(II) complexes containing pyca type ligands, which occur in solution as a mixture of *cis* and *trans* isomers, the

Table 2
Selected ^1H and ^{31}P NMR data for the complexes [NiR(N–O)L]

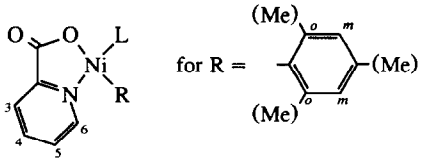

Complex	^1H NMR					^{31}P NMR
	R		pyridine ring		L	
	Me	*o*-H	H4	H6		
1a	2.62(3)s	7.44d(J_{HH} = 7.5)	6.05dd(J_{HH} = 6.5)	7.92d(J_{HH} = 7.6)		26.22
1b	2.47(3)s	7.42d(J_{HH} = 6.2)	6.0dd(J_{HH} = 6.1)	7.95d(J_{HH} = 7.1)	CH_2 2.68m	26.1
1c	2.73(3)s	7.40d(J_{HH} = 7.2)	6.02dd(J_{HH} = 4.0; 1.5)	7.88d(J_{HH} = 7.5)	*Me* 1.02d(J_{PH} = 10.2)	23.49(12.02)
1d	2.69(3)s	7.28d(J_{HH} = 7.2)	6.04dd(J_{HH} = 4.2; 1.3)	7.90d(J_{HH} = 7.6)	Me_1 0.87d(J_{PH} = 10.4) Me_2 1.15d(J_{PH} = 10.4)	0.69
1e	3.07(3)s	7.76t(J_{HH} = 3.9)	6.02dd(J_{HH} = 6.4)	7.89d(J_{HH} = 7.6)		30.28
1f		7.30(2)d(J_{HH} = 7.0)	6.05dd(J_{HH} = 5.8)	7.91d(J_{HH} = 7.6)		
1g	2.13(3)s	7.30(2)d(J_{HH} = 6.9)	6.08dd(J_{HH} = 6.0)	7.91d(J_{HH} = 7.6)		24.09
1h	2.82(6)s 2.26(3)s	(*m* – H) 6.65(2)s	6.05dd(J_{HH} = 6.7)	7.92d(J_{HH} = 7.6)	*Me* 0.91d(J_{PH} = 9.6)	9.19
2	2.94(6)s 2.21(3)s	(*m* – H) 6.58(2)s	5.90dd(J_{HH} = 6.4)	7.58d(J_{HH} = 5.6)	*Me* 0.78d(J_{PH} = 9.4)	5.7

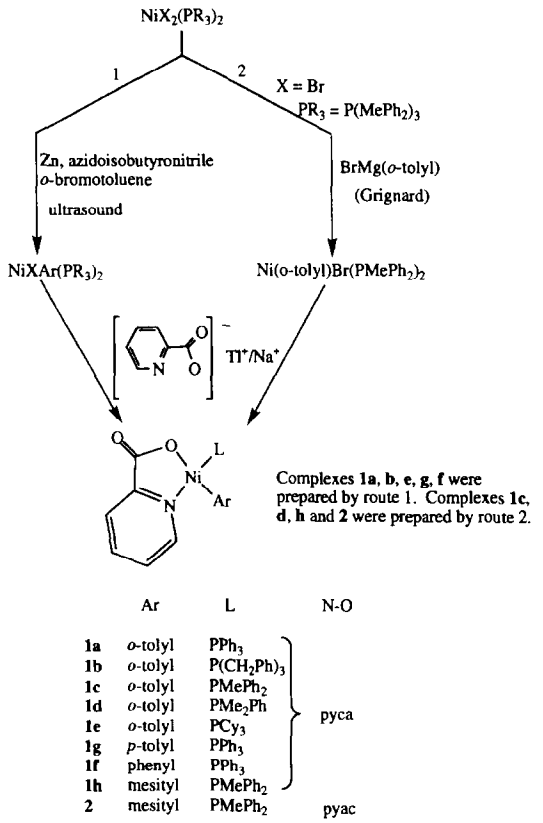

Scheme 1. Preparative routes for the complexes [Ni(R)(N–O)(L)].

square planar chelate nickel(II) complexes of type **1**, and **2** give only one observable isomer in solution, probably the isomer with the N *trans* P structure. The solid state structures (N *trans* P) were confirmed by X-ray.

3.2. Characterization of the complexes [Ni(aryl)(N–O)PR_3]

All complexes exhibited characteristic strong bands in their IR spectra in the region 1668–1662 cm^{-1}, which are assigned to (C=O) stretching vibrations. Peaks around 1480 cm^{-1} are assigned to aromatic (C–C) vibrations, while peaks at 1606 and 1604 cm^{-1} are assigned to pyridine ring deformations [16]. Compared with free N–O ligand, an increase in frequency of 14–18 cm^{-1} for the pyridine ring deformations on coordination of the chelate ligand confirms the expected coordination through the pyridyl nitrogen [17].

Selected ^1H and ^{31}P NMR data for the complexes of type **1** and **2** are shown in Table 2. Complexes where R = *o*-tolyl and *p*-tolyl show singlets between δ 2.12 ppm and δ 3.07 ppm. The peaks correspond to the tolyl methyl groups in the *ortho* and *para* positions respectively. The mesityl–methyl protons for the complexes **1h** and **2** are split into two singlets; δ 2.26 ppm (three protons) and δ 2.82 ppm (six protons) for **1h** and δ 2.21 ppm (three protons) and δ 2.94 ppm (six protons) for **2**. The methyl group of $PMePh_2$ in **1c** appears as a doublet at δ 0.91 ppm due to coupling with ^{31}P. For complex **1b**, L = $P(CH_2Ph)_3$, a complex multiplet at δ 2.69 ppm was attributed to the benzylic protons. The presence of two doublets at δ 0.87 and 1.15 ppm (coupling constant J_{PH} = 10.4 Hz) for complex **1d** (L = PMe_2Ph), indicates that the two methyl groups on the phosphine differ in their environment [2,13] and that rotation of the phosphine is restricted. Importantly, it also indicates that under the conditions of the NMR experiment no phosphine dissociation occurs.

Table 3
Activities of the complexes [Ni(aryl)(N–O)(PR_3)] for oligomerisation of ethylene [a]

Complex	Solvent	Turnover number [b] (TON)	Linearity (%)	α-Olefin (%)
Ni(*o*-tolyl)(pyca)(PPh_3) (**1a**) [c]	toluene	1150(±200)	96	63
	benzene	1300(±100)	92	63
	Cl-benzene	270(±10)	90	59
	methanol	0		
Ni(*o*-tolyl)(pyca)($P(CH_2Ph)_3$) (**1b**)	toluene	900(±200)	84	51
	benzene	1800(±300)	85	54
Ni(*o*-tolyl)(pyca)($PMePh_2$) (**1c**)	toluene	200(±50)	94	74
	benzene	420(±40)	94	76
Ni(*o*-tolyl)(pyca)(PMe_2Ph) (**1d**)	toluene	60	99	87
Ni(*o*-tolyl)(pyca)(PCy_3) (**1e**)	benzene	950(±200)	92	69
Ni(phenyl)(pyca)(PPh_3) (**1f**)	toluene	0		
Ni(mesityl)(pyca)($PMePh_2$) (**1h**)	toluene	6	98	71
Ni(mesityl)(pyac)($PMePh_2$) (**2**)	toluene	trace		

[a] Reaction conditions: approximately 50 mg of catalyst dissolved in 10–15 ml solvent; temperature 80°C, ethylene pressure 40 bar at room temperature (approximately 50 bar at operating temperature initially). The percentage linear α-olefin was determined by GC from the C_6 cut.
[b] TON is the total number of catalyst turnovers, i.e. moles of ethylene consumed per mole of catalyst (the quantity of oligomers obtained is calculated from GC using nonane as an internal standard). Values are probably underestimates due to some loss of volatile components.
[c] Traces of polyethylene are observed with this catalyst in toluene and benzene. In chlorobenzene 1.1–1.3 g of polyethylene are produced.

The aromatic region of the ^1H NMR spectra is complex. However, two-dimensional ^1H NMR experiments (COSY) assisted in assigning characteristic peaks in the aromatic region of pyca. The assignment of proton H^4 was based on the notable absence of a multiplet at around δ 6.02 ppm in the spectra of complexes for which there was a substituent in the *para* position of the pyridyl ligand. For compounds in which H^4 is present, the proton resonates upfield compared with other pyridyl protons and in well-resolved spectra a multiplet is observed due to long range *meta* coupling. Another distinctive feature of the pyridyl ring is the unusually high chemical shift of the *ortho* proton H^6 (as a doublet around δ 7.9 ppm) due to the strong deshielding effect that the nitrogen exerts on the *ortho* position [18]. Although *meta* coupling between H^4 and H^6 is not always resolved, the cross peaks on the contour plot clearly show *J*-coupling between H^4 and H^6. These pyridyl protons are very sensitive to changes in the ring environment and can be used to monitor bonding and reaction behaviour.

By comparing NMR spectra for complexes where R = *o*-tolyl and R = mesityl it was possible to assign a doublet between δ 7.3 ppm and δ 7.4 ppm (J_{HH} = 6–7 Hz), which is only present in complexes with the *o*-tolyl ligand, to the *ortho* proton of the coordinated tolyl group.

3.3. Catalytic results

Complexes of the type [MR(pyca)L] (where M = Pt(II) and Pd(II); L = monodentate Lewis base) were found to exhibit unusual lability. For these complexes carbonylation was considered to go via a dissociative pathway in which the ligand L is replaced by incoming CO [4,7]. However, by careful selection of ring substituents, an alternative route, via initial displacement of the pyridine ring of the pyca ligand, may be induced [9]. Similarly, intramolecular alkene insertion was found to progress via partial dissociation of the chelate ligand, promoted by the initial coordination of the alkene [8]. These results suggested to us that the related nickel complexes may exhibit catalytic activity in C–C coupling reactions. Subsequently the arylnickel complexes of pyca and pyac were prepared and found to give single component catalysts for the oligomerisation of ethylene.

Catalytic results are listed in Tables 3 and 4. The catalysts display low to moderate activity for the oligomerisation of ethylene to linear higher olefins. There is very little branching in the products, indicating that generally only ethylene (and not product olefin) is inserted into the growing chain. The occasional presence of small amounts (around 1–2%) of 2-ethylbutenes in the products, however, indicates that a small amount of 1-butene must insert into the nickel–ethyl bond. The percentage of α-olefin, calculated from the hexenes cut, ranged from approximately 50 to 90%. The activity and in particular the percentage of α-olefins in the product is extremely dependent on the phosphine associated with the complex. This marked influence exerted by the monodentate phosphine in nickel based catalysis is well known [19,20]. The extent of phosphine control would strongly suggest that the active catalytic species contains coordinated phosphine.

Of particular interest is the effect of adding free triphenylphosphine to the catalyst systems. Even small excesses of free phosphine have a dramatic effect on the distribution of ethylene oligomers. The effect is most clearly demonstrated for the catalyst [Ni(*o*-tolyl)(pyca)-(PPh_3)], and is shown in Table 5. The activity of the catalyst is also somewhat affected by excess PPh_3; addition of 1 equivalent of PPh_3 leads to a decrease in activity by a factor of 2–3. However, the total number of turnovers remains constant, within experimental error, for Ni: free PPh_3 ratios up to 1:1. For high concentrations of free PPh_3 (i.e. PPh_3: Ni ratio 5:1) there is a significant decline in total turnovers; probably due to effective blocking of coordination sites by PPh_3. The most notable effects of added phosphine are a sharp increase in the percentage of C_4–C_{10} olefins produced (from 75 to around 100%) on adding up to 1 equivalent of free PPh_3 and a concomitant increase in the product linearity to nearly 100%. The amount of α-olefin also increases somewhat to approximately 75% (from 63%). A consideration of the possible active catalyst and of

Table 4
Oligomer distributions for the oligomerisation of ethylene for selected [Ni(aryl)(N–O)(PR_3)] complexes

Carbon No.	Distribution (wt.%)		
	Ni(*o*-tolyl)(N–O)(PPh_3) (**1a**)	Ni(*o*-toyl)(N–O)[$P(CH_2Ph)_3$ (**1b**)	Ni(*o*-tolyl)(N–O)(PCy_3) (**1c**)
4	30.6	41.7	53.4
6	24.2	20.7	22.3
8	16.1	17.5	11.6
10	9.8	8.2	6.4
12	7.3	5.4	3.2
14	4.7	4.7	1.7
16	3.0	1.7	0.9
18	1.4	0.0	0.5

Table 5
Oligomerisation of ethylene in the presence of excess PPh_3 [a]

Ni: free PPh_3	TON [b] (in first hour)	TON (over 12 h)	C4–C10 olefins (%)	Linear α-olefins (%)
1:0	310±75	1150±200	75±4	63±3
1:0.5	140±5	1200±300	94±2	71±2
1:1	120±15	1000±300	98±2	75±1
1:5	—	200±70	~100	~77 [c]
1:10	—	170±50	~100	[c]

[a] Reaction conditions: approximately 50 mg of catalyst [Ni(*o*-tolyl)(pyca)PPh_3] dissolved in 10–15 ml solvent (toluene); temperature 80°C; ethylene pressure 40 bar at room temperature (catalytic runs were carried out for 12 h). Each result is the mean of at least three runs.
[b] TON is the total number of catalyst turnovers, i.e. moles of ethylene consumed per mole of catalyst.
[c] The low yield of products made it impossible to obtain a clear analysis of the product.

the overall mechanism for oligomerisation may assist in rationalising these observations.

3.4. Mechanistic considerations

GC-MS analyses of the products from a number of the catalyst systems show the presence of approximately stoichiometric amounts of the primary insertion products; vinylic–aryl compounds and aryl species resulting from double insertions of ethylene (Scheme 2). The complex [Ni(*o*-tolyl)(pyca)(PPh_3)] gives *o*-vinyltoluene and [Ni(mesityl)(pyca)(PPh_3)] gives vinylmesitylene and some butenylmesitylene as products. These products are consistent with the generally held Cossee type mechanism for olefin oligomerisation (as outlined in Scheme 2) [21].

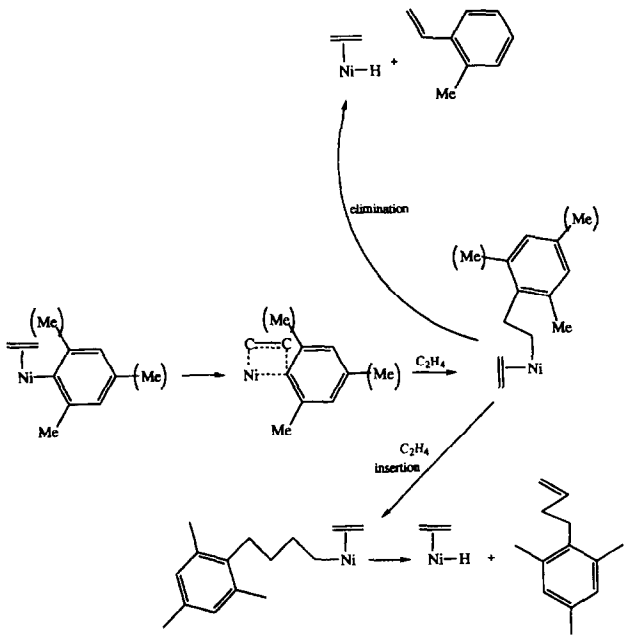

Scheme 2. Possible mechanism for ethylene insertion in the presence of excess PPh_3.

The Cossee mechanism proposes that chain growth occurs by olefin insertion into a metal–hydride (or alkyl) bond. Chain termination is generally thought to occur by β-hydrogen transfer or abstraction. It is commonly felt that for d_8 metal complexes insertion of a coordinated olefin occurs from a four-coordinate intermediate (i.e. via a dissociative mechanism). An alternative insertion mechanism is the associative route in which insertion occurs from a five-coordinate intermediate, without prior ligand displacement.

We have been unable to find any evidence for either phosphine dissociation or exchange, or hemilability of the N–O ligand for the complexes **1a–h** and **2**. Treatment of [Ni(*o*-tolyl)(pyca)PPh_3], complex **1a**, with the phosphine trap MeI at room temperature (22°C) gave no reaction (even after 2 h), indicating that phosphine dissociation did not occur under these conditions [22], and reaction of **1a** with excess PPh_3, at temperatures up to 80°C, did not result in any shift or broadening of the ^{31}P NMR peak for the coordinated phosphine. Some broadening of the free PPh_3 was evident, however, there was no shift in the peak position. ^{31}P NMR and ^1H NMR studies of **1a** in the presence of ethylene at temperatures up to 60°C, although confirming that oligomerisation was occurring, provided no evidence for dissociation or displacement of the coordinated phosphine or partial dissociation of pyca; signals for the protons in the 4- and 6-positions of the pyridine ring show little or no change. Ethylene oligomers were identified by ^1H NMR and the peak due to dissolved ethylene gradually disappeared on reaction at 60°C.

In several important studies the consequence of excess ligand and the relationship to possible insertion pathways has been considered. Garrou and Heck [23] undertook extensive kinetic and NMR studies on carbonylation reactions of square planar, hydrocarbyl bisphosphine complexes of Pt(II), Pd(II) and Ni(II) and found that excess ligand resulted in significantly depressed reaction rates. Rates decreased with increasing amounts of added ligand until a constant limiting rate was obtained. The authors reasoned that two reaction pathways occur, both going via an initial five-coordinate, trigonal bipyramid intermediate (**III**, Scheme 3), consisting of the original complex plus coordinated CO. One pathway was the favoured dissociative route, which was severely repressed by adding excess phosphine (excess ligand prevents dissociation of the coordinated phosphine — enough excess phosphine led to complete suppression of this path) and the second was the alternative associative route which is not inhibited by excess ligand.

In a later study looking at intramolecular acetylene and olefin insertion into palladium–carbon bonds, Samsel and Norton [24] have proposed a dissociative route

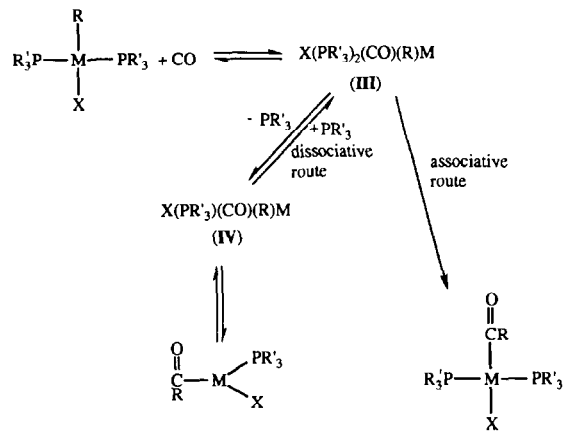

Scheme 3. Dual pathway mechanism proposed by Garrou and Heck [21].

for the insertion process and have used the effect of excess ligand to provide support for their proposal. They suggested that in the absence of free ligand insertion takes place from a four-coordinate intermediate. This route is severely inhibited by excess ligand; the dissociation equilibrium (Eq. (1)) is forced to the left, preventing the formation of a vacant site for the coordination of unsaturated species and leading to a dramatic reduction in the rate of insertion (the rate decreases by a factor of 50 on addition of 0.5 equivalents of PPh_3). Samsel and Norton point out that such a large suppression of the insertion process cannot be explained by an associative mechanism (Eq. (2)), where insertion takes place from a five-coordinate intermediate (**VI**). At most, the addition of 0.5 equivalents of free PPh_3 can tie up 50% of the initial complex to give the unproductive species **V** and hence only decrease the rate by a factor of two. From a ^{31}P NMR investigation, Samsel and Norton also noted a slow associative exchange process between free and coordinated PPh_3.

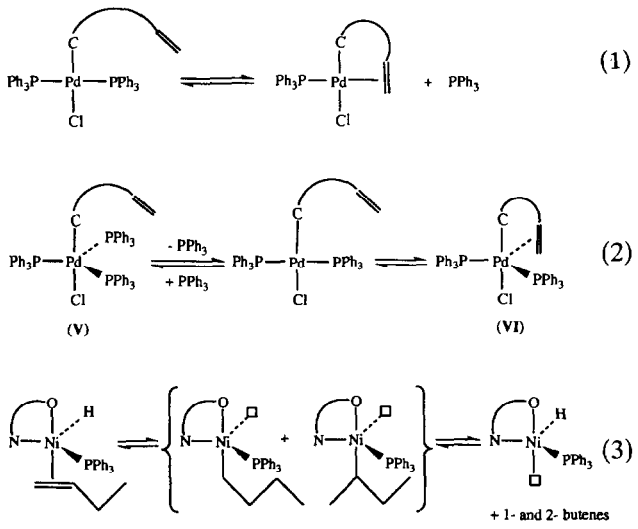

In the present study the complete lack of any NMR evidence for ligand exchange or dissociation, even on warming, suggests ligand dissociation/displacement is not a facile route for these nickel complexes. Therefore, in accord with the previous studies, a five-coordinate intermediate, i.e. associative insertion mechanism, seems to be a possibility [23,24]. However, as we were unable to emulate the relatively severe catalytic conditions in the NMR tube, the failure to observe any evidence of ligand lability does not rule out ligand dissociation or displacement as a pathway for insertion.

Notwithstanding the large changes in product distribution observed in the presence of excess ligand, relatively small changes in catalyst activity are observed (0.5 equivalents of excess PPh_3 decreased the activity by a factor of approximately 2). This "stoichiometric" decrease in activity is consistent with a pathway in which half the molecules form a five-coordinate complex of type **VII** (Scheme 4) with no site available for ethylene coordination and thus are unable to catalyse the insertion process. It therefore seems possible that an associative route may be the preferred catalytic pathway for these complexes. Furthermore, the propensity of nickel to form five-coordinate complexes is also well known, and reactions involving nickel complexes often involve five-coordinate species as intermediates or isolable complexes [25].

Modifications to the product distribution on addition of free ligand are not easily explained. However, chain branching and product isomerisation in ethylene oligomerisation can only occur if product olefins recoordinate instead of ethylene substrate (coordination and insertion of ethylene yields only linear α-olefins). Recoordination of product olefins, already limited in the presence of a large excess of ethylene (ethylene oligomerisation is also substantially faster than that of higher olefins on thermodynamic grounds [26]), is now further blocked by competition with free ligand.

On the basis of these results Scheme 4 is suggested as a possible oligomerisation mechanism. However, the evidence is limited and a dissociative pathway cannot be precluded.

3.5. *Solid state structures of Ni(mesityl)(pyca)PMePh$_2$ and Ni(mesityl)(pyac)PMePh$_2$*

Selected bond distances and angles are provided in Table 6 and coordinates for the non-hydrogen atoms are given in Tables 7 and 8. Projections oblique and normal to the coordination planes are shown in Figs. 1(a)–1(d).

The effect of changing from a five-membered chelate ring [in the complex Ni(mesityl)(pyca)$PMePh_2$, **1h**] to a six-membered ring [in Ni(mesityl)(pyac)$PMePh_2$, **2**] is clearly seen from the structures of the complexes (Fig. 1).

Table 6
Coordination geometry (distances in angstroms, angles in degrees) for the complexes Ni(mesityl)(pyca)($PMePh_2$) and [Ni(mesityl)(pyac)($PMePh_2$)]

Ni–P	2.148(2), [2.162(2)]	N–O(21)	1.911(5), [1.932(3)]
Ni–N	1.926(6), [1.951(3)]	Ni–C(01)	1.865(8), [1.890(4)]
P–Ni–N	176.6(2), [169.8(1)]	O(21)–Ni–C(01)	177.2(3), [173.4(2)]
P–NiO(21)	92.1(2), [88.4(1)]	N–Ni–O[21]	84.6(2), [90.3(1)]
P–Ni–C(01)	89.7(2), [89.7(1)]	N–Ni–C(01)	93.6(3), [92.7(2)]
Ni–P–C(111)	110.5(3), [119.6(2)]	Ni–N(1)–C(2)	111.5(5), [117.3(3)]
Ni–P–C(121)	112.6(2), [114.6(1)]	Ni–N(1)–C(6)	128.8(5), [125.0(3)]
Ni–P–C(131)	119.7(3), [109.7(2)]	C(2)–N(1)–C(6)	119.7(6), [117.8(4)]
C(111)–P–C(121)	105.1(4), [104.0(2)]	Ni–O(21)–C(21)	114.9(5), [121.8(3)]
C(111)–P–C(131)	105.5(4), [104.4(2)]	N(1)–C(2)–C(21/20)	114.8(6), [117.9(4)]
C(121)–P–C(131)	102.1(4), [102.9(2)]		

In the pyca complex the array NiPN(1)O(2)C(01) is effectively planar [χ^2 45; atom deviations δ being −0.002(1), 0.000(1), 0.002(7), 0.020(6), 0.046(8) Å respectively]; in the pyac complex significant non-planarity is found [χ^2, 7×10^3; δ −0.025(1), 0.029(2), 0.269(4), −0.076(4), −0.182(6) Å respectively], the effect perhaps best being described as a twist of the NiN(1)C(01) array relative to NiP(1)O(21). The two complexes differ in the disposition of the pyridine moiety vis-a-vis the above "coordination planes" — in the pyca complex the NC_5 plane [δ Ni, 0.02(1) Å] is effectively coplanar with the carboxylate CCO_2 plane [δ Ni, 0.133(9) Å], the interplanar dihedral angle being 2.4(7)°, and the two planes making angles of 4.0(7)° and 2.4(7)° with the coordination plane. In the pyac complex, the dihedral angle between the NC_5 and CCO_2 planes is 55.5(2)°, and their angles to the coordination

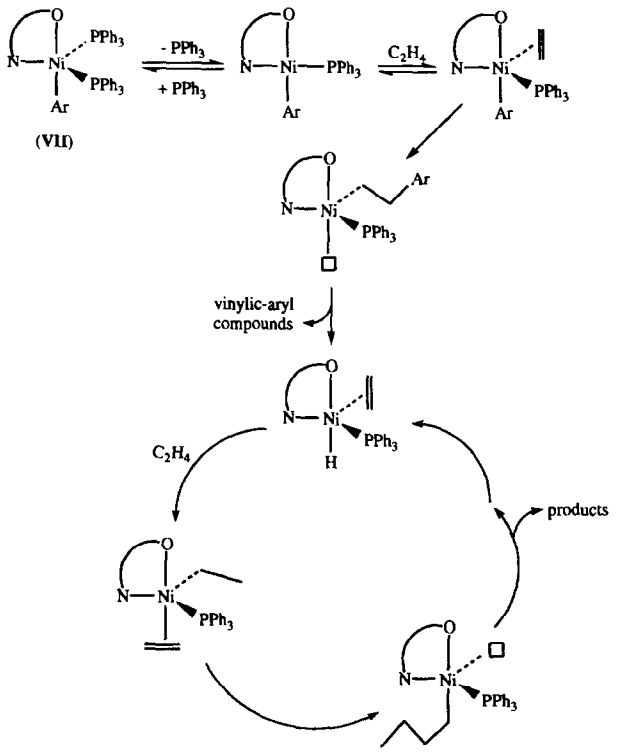

Scheme 4. Proposed mechanism for ethylene oligomerisation for the catalysts [NiR(pyca)PR'_3].

Table 7
Non-hydrogen positional and isotropic displacement parameters [Ni(mesityl)(pyca)($PMePh_2$)]

Atom	x	y	z	U_{eq} Å^2
Ni	0.71678(6)	0.6995(1)	0.36689(4)	0.0483(4)
P(1)	0.7643(1)	0.5709(3)	0.45608(9)	0.0554(9)
C(111)	0.7865(5)	0.7090(9)	0.5240(3)	0.060(3)
C(112)	0.8710(6)	0.707(1)	0.5723(4)	0.081(4)
C(113)	0.8825(7)	0.813(1)	0.6238(4)	0.107(5)
C(114)	0.8140(7)	0.916(1)	0.6265(4)	0.103(5)
C(115)	0.7311(7)	0.919(1)	0.5811(5)	0.112(5)
C(116)	0.7184(6)	0.814(1)	0.5288(4)	0.090(4)
C(121)	0.6773(5)	0.4321(8)	0.4686(3)	0.053(3)
C(122) *	0.621(1)	0.461(2)	0.5081(7)	0.072(8)
C(123) *	0.553(1)	0.351(2)	0.5134(9)	0.09(1)
C(124)	0.5437(7)	0.215(1)	0.4839(6)	0.111(6)
C(125) *	0.595(2)	0.196(2)	0.442(1)	0.13(1)
C(126) *	0.662(2)	0.300(3)	0.435(1)	0.12(1)
C(122′) *	0.681(1)	0.379(2)	0.5332(8)	0.073(8)
C(123′) [b]	0.614(1)	0.270(2)	0.542(1)	0.10(1)
C(125′) *	0.546(1)	0.252(2)	0.428(1)	0.10(1)
C(126′) *	0.609(1)	0.367(2)	0.4142(9)	0.085(9)
C(131)	0.8688(6)	0.444(1)	0.4709(4)	0.092(4)
N(1)	0.6676(4)	0.8179(7)	0.2883(3)	0.063(3)
C(2)	0.5836(5)	0.881(1)	0.2850(4)	0.069(4)
C(21)	0.5471(5)	0.8450(9)	0.3419(4)	0.060(3)
O(21)	0.5995(3)	0.7511(6)	0.3829(2)	0.059(2)
O(22)	0.4702(4)	0.8991(7)	0.3433(3)	0.086(3)
C(3)	0.5349(8)	0.973(1)	0.2337(5)	0.137(6)
C(4)	0.5771(9)	0.998(2)	0.1828(5)	0.168(8)
C(5)	0.6613(7)	0.933(1)	0.1863(5)	0.121(6)
C(6)	0.7063(6)	0.841(1)	0.2393(4)	0.083(4)
C(01)	0.8319(5)	0.6596(8)	0.3503(3)	0.054(3)
C(02)	0.9069(5)	0.7713(9)	0.3700(4)	0.064(3)
C(021)	0.8955(7)	0.916(1)	0.4065(5)	0.102(5)
C(03)	0.9917(5)	0.7411(9)	0.3539(4)	0.069(4)
C(04)	1.0037(5)	0.611(1)	0.3183(4)	0.073(4)
C(041)	1.0944(7)	0.585(1)	0.3003(5)	0.116(6)
C(05)	0.9294(5)	0.502(1)	0.2983(4)	0.068(4)
C(06)	0.8471(5)	0.5231(9)	0.3148(4)	0.059(3)
C(061)	0.7662(6)	0.405(1)	0.2905(4)	0.080(4)

* Site occupancy factor 0.5

plane are 43.9(1)° and 52.0(1)° in opposite senses. Torsion angles N(1)–C(2)–C(20)–C(21) and C(2)–C(20)–C(21)–O(21) in the latter are −54.0(5)° and 56.0(5)° respectively. Despite the less agreeable planarity of the pyac/coordination plane in the latter complex (vis-a-vis the pyca analogue), the disposition appears to be associated with considerable strain relief in that part of the system, as evidenced by the changes in the angles at the nitrogen atom, C(2) and O(21); the *trans* angles about the Ni are less linear, however, and the six-membered ring of complex **2** is a severely distorted boat. To maintain essentially square planar coordination about the metal atom the carbons C2, C20 and C21 of the chelating ligand are bent well out of the NiPONC coordination plane, in particular C20 is bent sharply away from the plane (this can be readily observed in Fig. 1).

Although the phenyl ring C12n of the phosphine in the pyca complex is disordered over two sites, the phenyl groups of the phosphine clearly are directed to either side of the coordination plane. The methyl group is almost parallel with the coordination plane. In the pyac complex, however, the phosphine ligand is arranged with the phenyl groups of the phosphine pointing away from the bent chelate ring and the less sterically demanding methyl group is on the same side of the coordination plane as the bent ring. In the pyca complex the largest Ni–P–C angle is to C(131); in the pyac complex to C(111).

In both complexes the mesitylene ligand lies exactly at right angles to the NiPONC coordination plane [dihedral angles 89.6(2)°, 90.0(7)°; δ Ni, 0.12(1), 0.039(7) Å], minimising steric interactions between ligands. This arrangement of relatively bulky ligands (mesityl and

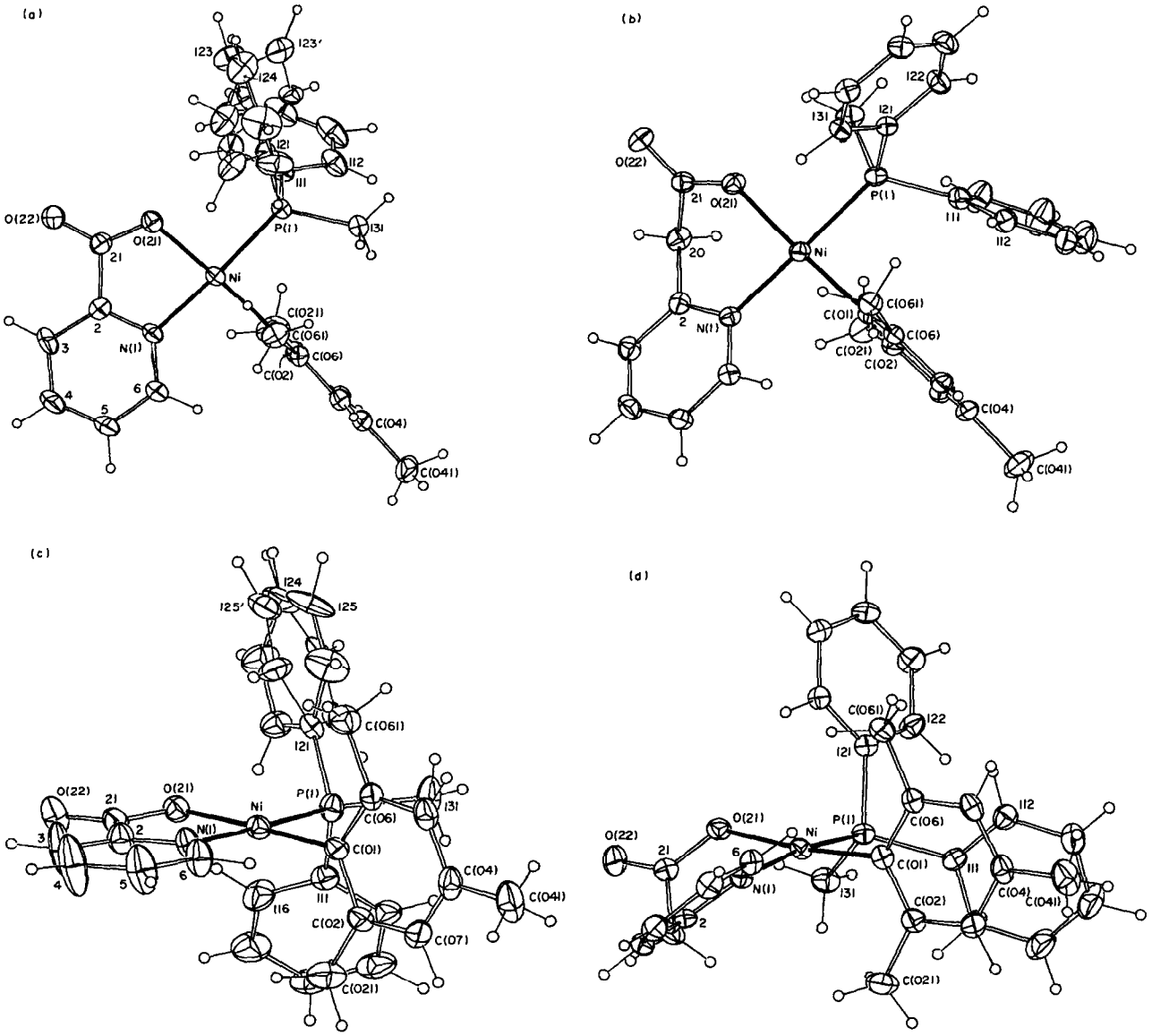

Fig. 1. Molecular projections oblique and normal to the coordination planes for the complexes Ni(mesityl)(pyca)$PMePh_2$ (a) and (c); Ni(mesityl)(pyac)$PMePh_2$ (b) and (d); 20% thermal ellipsoids are shown for the non-hydrogen atoms.

Table 8
Non-hydrogen positional and isotropic displacement parameters [Ni(mesityl)(pyac)($PMePh_2$)]

Atom	x	y	z	U_{eq} Å^2
Ni	0.39946(3)	0.67719(2)	0.07798(6)	0.0418(2)
P(1)	0.29566(6)	0.64322(4)	0.1206(1)	0.0429(4)
C(111)	0.2988(2)	0.5940(1)	0.2216(5)	0.048(2)
C(112)	0.3158(3)	0.5558(2)	0.1562(5)	0.056(2)
C(113)	0.3217(3)	0.5190(2)	0.2353(7)	0.076(2)
C(114)	0.3106(4)	0.5200(2)	0.3799(7)	0.093(3)
C(115)	0.2956(4)	0.5576(2)	0.4456(6)	0.102(3)
C(116)	0.2889(3)	0.5944(2)	0.3668(6)	0.075(2)
C(121)	0.2408(2)	0.6297(1)	−0.0366(5)	0.042(2)
C(122)	0.1785(3)	0.6028(2)	−0.0291(5)	0.058(2)
C(123)	0.1363(3)	0.5941(2)	−0.1475(6)	0.067(2)
C(124)	0.1548(3)	0.6118(2)	−0.2760(5)	0.059(2)
C(125)	0.2161(3)	0.6389(2)	−0.2864(5)	0.054(2)
C(126)	0.2584(2)	0.6481(1)	−0.1661(5)	0.044(2)
C(131)	0.2315(3)	0.6769(2)	0.2200(5)	0.062(2)
N(1)	0.4902(2)	0.7124(1)	0.0727(4)	0.041(1)
C(2)	0.4851(2)	0.7518(2)	0.1282(5)	0.046(2)
C(20)	0.4098(3)	0.7662(1)	0.1803(5)	0.055(2)
C(21)	0.3479(3)	0.7622(2)	0.0686(5)	0.047(2)
O(21)	0.3391(2)	0.72479(9)	0.0158(3)	0.050(1)
O(22)	0.3097(2)	0.7930(1)	0.0361(4)	0.069(1)
C(3)	0.5479(3)	0.7780(1)	0.1348(5)	0.056(2)
C(4)	0.6163(3)	0.7645(2)	0.0820(6)	0.064(2)
C(5)	0.6206(3)	0.7248(2)	0.0214(6)	0.059(2)
C(6)	0.5580(3)	0.7001(1)	0.0200(5)	0.051(2)
C(01)	0.4554(2)	0.6276(1)	0.1191(5)	0.045(2)
C(02)	0.4805(2)	0.6188(1)	0.2574(6)	0.052(2)
C(021)	0.4643(3)	0.6491(2)	0.3766(6)	0.080(2)
C(03)	0.5221(3)	0.5822(2)	0.2841(6)	0.061(2)
C(04)	0.5417(3)	0.5542(2)	0.1775(7)	0.062(2)
C(041)	0.5896(3)	0.5156(2)	0.2112(7)	0.100(3)
C(05)	0.5185(3)	0.5631(1)	0.0412(6)	0.054(2)
C(06)	0.4751(2)	0.5988(1)	0.0113(5)	0.047(2)
C(061)	0.4491(3)	0.6063(1)	−0.1389(6)	0.057(2)

$PMePh_2$) about the nickel centre might be expected to limit the access of approaching substrate molecules and may also destabilise the five-coordinate intermediates necessary for an associative insertion mechanism. Steric constraints about the metal centre therefore would be expected to favour displacement of a ligand on coordination of ethylene to nickel.

It is interesting to note that the metal–ligand bonds for complex **2** are all slightly longer than those for complex **1h** [Δ Ni–P = 0.014(2); Δ Ni–N = 0.025(5); Δ Ni–O = 0.021(4); Δ Ni–C = 0.025(7)]. The differences are small but consistent, but may be an artefact of the consequences of disorder transmitted throughout the structure as noted above. The expected concomitant weakening of the metal to ligand bonding is not reflected in the catalytic behaviour of **2**. Surprisingly, complex **2** gives rise to a catalyst with one of the lowest activities observed for this group of catalysts. However, in accord with previous data, this may simply reflect that ligand dissociation is not the insertion pathway for these catalysts.

Acknowledgements

We are indebted to the Australian Research Council for financial support and for providing an Australian Postgraduate Award for S.Y.D. and a Research Associateship for H.J. We would also like to acknowledge the support and assistance of Professor Dr. W. Keim (RWTH, Aachen) in allowing S.Y.D. to spend four months working in his laboratories gaining valuable experience. The assistance of Mr. Evan Peacock (CSL, University of Tasmania) with the analysis of NMR spectra is also gratefully acknowledged.

References

[1] G.K. Anderson and G.J. Lumetta, *Organometallics, 4* (1985) 1542.
[2] G.P.C.M. Dekker, C.J. Elsevier, K. Vrieze and P.W.N.M. van Leeuwen, *Organometallics, 11* (1992) 1598.
[3] K.J. Cavell, H. Jin, B.W. Skelton and A.H. White, *J. Chem. Soc., Dalton Trans.*, (1992) 2923.
[4] H. Jin and K.J. Cavell, *J. Chem. Soc., Dalton Trans.*, (1994) 415.
[5] G.P.C.M. Dekker, A. Buijs, C.J. Elsevier, K. Vrieze, P.W.N.M. van Leeuwen, W.J.J. Smeets, A.L. Spek, Y.F. Wang and C.H. Stam, *Organometallics, 11* (1992) 1937.
[6] A. Sen, *Acc. Chem. Res., 26* (1993) 303.
[7] H. Jin, K.J. Cavell, B.W. Skelton and A.H. White, *J. Chem. Soc., Dalton Trans.*, (1995) 2159.
[8] K.J. Cavell and H. Jin, *J. Chem. Soc., Dalton Trans.*, (1995) 4081.
[9] K.J. Cavell, J.L. Hoare and R. Hecker, accepted for publication, *J. Chem. Soc., Dalton Trans.*
[10] H.-F. Klein and T. Wiemer, *Inorg. Chim. Acta, 189* (1991) 267.
[11] R.G. Hayter and F.S. Humiec, *Inorg. Chem., 4* (1965) 1701.
[12] L.M. Venanzi, *J. Chem. Soc.*, (1958) 719.
[13] S.R. Hall, H.D. Flack and J.M. Stewart (eds.), *The XTAL 3.2 Reference Manual*, Universities of Western Australia, Geneva and Maryland, 1992.
[14] M. Zembayashi, K.J. Tamao, J.-I. Yoshida and M. Kumada, *Tetrahedron Lett., 47* (1977) 4089.
[15] J.R. Moss and B.L. Shaw, *J. Chem. Soc. A*, (1966) 1793.
[16] D.P. Madden and S.M. Nelson, *J. Chem. Soc. A*, (1968) 2342.
[17] A. Hessler, J. Fisher, S. Kuchen and O. Stelzer, *Chem. Ber., 127* (1994) 481.
[18] A.J. Boulton and A. McKillop, in *Comprehensive Heterocyclic Chemistry*, Vol. 2, Pergamon Press, Sydney, pp. 9–11.
[19] B. Bogdanovic, *Adv. Organomet. Chem., 17* (1979) 105.
[20] (a) R. Abeywickrema, M.A. Bennett, K.J. Cavell, M. Kony, A.F. Masters and A.G. Webb, *J. Chem. Soc., Dalton Trans.*, (1993) 59; (b) K.J. Cavell, *Aust. J. Chem., 47* (1994) 769.
[21] E.J. Arlman and P. Cossee, *J. Catal., 3* (1964) 99.
[22] V. De Felice, A. De Renzi, D. Tesauro and A. Vitagliano, *Organometallics, 11* (1992) 3669.
[23] P.E. Garrou and R.F. Heck, *J. Am. Chem. Soc., 98* (1976) 4115.
[24] E.G. Samsel and J.R. Norton, *J. Am. Chem. Soc., 106* (1984) 5505.
[25] S.A. Macgregor, Z. Lu, O. Eisenstein and R.H. Crabtree, *Inorg. Chem., 33* (1994) 3616 and references cited therein.
[26] J.B. Pedley, R.D. Naylor and S.P. Kirby, *The Thermochemical Data of Organic Compounds*, Chapman and Hall, London, 2nd edn., 1986.